



From Molecules to Processes: Molecular Simulations Applied to the Design of Simulated Moving Bed for Ethane/Ethylene Separation

Journal:	<i>The Canadian Journal of Chemical Engineering</i>
Manuscript ID:	CJCE-12-0551.R1
Wiley - Manuscript type:	Article
Date Submitted by the Author:	n/a
Complete List of Authors:	<p>Granato, Miguel; Faculdade de Engenharia da Universidade do Porto, LSRE - Laboratory of Separation and Reaction Engineering – Associate Laboratory LSRE/LCM</p> <p>Martins, Vanessa; Faculdade de Engenharia da Universidade do Porto, LSRE - Laboratory of Separation and Reaction Engineering – Associate Laboratory LSRE/LCM</p> <p>Santos, João; Faculdade de Engenharia da Universidade do Porto, LSRE - Laboratory of Separation and Reaction Engineering – Associate Laboratory LSRE/LCM</p> <p>Jorge, Miguel; Faculdade de Engenharia da Universidade do Porto, LSRE - Laboratory of Separation and Reaction Engineering – Associate Laboratory LSRE/LCM</p> <p>Rodrigues, Alírio; Faculdade de Engenharia da Universidade do Porto, LSRE - Laboratory of Separation and Reaction Engineering – Associate Laboratory LSRE/LCM</p>
Keywords:	Zeolite 13X, Ethane/Ethylene, Simulated Moving Bed, Molecular Simulation, Monte Carlo

SCHOLARONE™
Manuscripts

1
2
3
4 **From Molecules to Processes: Molecular Simulations Applied**
5
6
7 **to the Design of Simulated Moving Bed for Ethane/Ethylene**
8
9
10 **Separation**
11

12 *Miguel Angelo Granato^{§*}, Vanessa Duarte Martins[§], João Carlos Santos[§]*

13
14
15 *Miguel Jorge[§], and Alírio Egídio Rodrigues[§]*
16

17
18 [§] LSRE - Laboratory of Separation and Reaction Engineering – Associate Laboratory
19 LSRE/LCM, Faculdade de Engenharia, Universidade do Porto, Rua Dr. Roberto Frias.
20
21
22 4200-465 - Porto, Portugal
23
24

25
26 * To whom correspondence should be addressed: Phone +351 22 508 1578; Fax: +351
27
28 22 508 1674. E-mail: mgranato@fe.up.pt
29
30

31
32 **Abstract**
33
34

35 This paper presents results of a modelling study on the separation of ethane/ethylene
36 mixture by selective adsorption on zeolite 13X in a Simulated Moving Bed (SMB) unit.
37 Propane and *n*-butane are evaluated as desorbent candidates. The study encompasses
38 molecular simulation calculations for determination of adsorption parameters, whose
39 results will then be used in a mathematical model for evaluating the performance of an
40 SMB unit. This work is entirely done *in silico*, by using available force field parameters
41 for the molecular simulations part, and reliable mathematical models for the SMB part.
42 Experimental data are solely used for comparison with the molecular simulation results,
43 which are subsequently expanded to calculate adsorption properties for separating the
44 mixtures, without further experimental work. The separation regions of an SMB unit
45 operating with zeolite 13X for ethane/ethylene separation, using propane and *n*-butane
46
47
48
49
50
51
52
53
54
55
56
57
58
59
60

1
2
3 as desorbents, were obtained by simulation at 110 kPa and at four different
4
5 temperatures: 298, 323, 348 and 373 K. For each desorbent, an operating point was
6
7 selected and the size of the required unit was presented for the complete separation of
8
9 the two components of the mixture.
10

11 12 13 **Keywords**

14
15 Zeolite 13X; Ethane; Ethylene; Simulated Moving Bed; Molecular Simulation; Monte
16
17 Carlo
18
19

20 21 **1. Introduction**

22
23 Ethylene (ethene) is the major worldwide industrial feedstock, one of the most
24
25 important raw materials for the chemical industry with an annual production of more
26
27 than 25 million tons in the United States (Kirk-Othmer, 1991). Separation of
28
29 paraffin/olefin mixtures, in particular ethane/ethylene and propane/propylene, requires
30
31 huge distillation columns operated at a very high reflux ratio, one of the most energy
32
33 consuming processes in the chemical industry (Rege *et al.*, 1998). Alternative
34
35 technologies are Simulated Moving Bed (SMB) and Vacuum Swing Adsorption (VSA).
36
37 The Simulated Moving Bed (SMB) technology comes from the early 1960's, with its
38
39 first important industrial implementation of the Sorbex process by UOP. Since then, it
40
41 has been successfully applied, first to various large petrochemical separations, including
42
43 *p*-xylene separation from its C8 isomers, olefin/paraffin separation, and more recently in
44
45 the pharmaceutical and fine chemical industries (Sá Gomes *et al.*, 2008). The Sorbex
46
47 process operates mostly in the liquid phase by employing two separating agents: the
48
49 eluent (or desorbent) and the adsorbent. The eluent can either be a gas or a liquid. The
50
51 extract and the raffinate (products) are diluted with the eluent and additional separation
52
53 steps, by flash or fractional distillation, are required to yield the pure products.
54
55
56
57
58
59
60

1
2
3 However, the Sorbex process can also be used for gas phase separations where a vapour
4 or a supercritical fluid, typically CO₂, is used as eluent. Mazzotti and co-workers
5 developed a six-port vapour phase SMB pilot plant for the separation of an
6 *n*-pentane/iso-pentane mixture using *n*-heptane as desorbent and 5A-Zeolite as
7 adsorbent. They reported a higher separation efficiency in a vapour-phase SMB unit
8 compared to the liquid phase separation (Mazzotti *et al.*, 1995). Relevant references to
9 the SMB application in the separation of propylene/propane mixtures are found in the
10 literature (Rao *et al.*, 2005; Cheng and Wilson, 2001). Rao and collaborators reported
11 results for this separation using silica gel as adsorbent in a moving-port system which,
12 when embedded into a fixed bed, facilitates the continuous movement of the port along
13 the bed for the injection and withdrawal of a fluid. The parametric study indicates that
14 high purity products and a higher productivity by an order of magnitude can be
15 achieved with simulated moving-beds compared to the fixed beds (Rao *et al.*, 2005).
16
17
18
19
20
21
22
23
24
25
26
27
28
29
30

31 In considering the ethane/ethylene separation by SMB, a suitable desorbent is a
32 fundamental issue. The choice of an adequate desorbent for the separation of
33 ethane/ethylene by gas phase SMB should consider the subsequent distillation step in
34 order to concentrate the extract/raffinate, and to recover the desorbent. **The difference**
35 **between the boiling point of the desorbent and that of the raffinate (or the extract), and**
36 **the presence or not of azeotropes are of key importance for the efficiency of the**
37 **distillation.** Propane and *n*-butane are proposed as candidate desorbents for separation of
38 the ethane/ethylene mixture, and this is tested using predictive simulations with little
39 input from experiment. At **101.3 kPa** (1 atm), ethane has a boiling point of -89 °C, and
40 ethylene has one of -103.7 °C. The boiling point of *n*-butane is -0.5 °C and that of
41 propane is -42.1 °C, and thus both desorbents would be adequate for further separation
42 by distillation.
43
44
45
46
47
48
49
50
51
52
53
54
55
56
57
58
59
60

1
2
3 Normally the choice of desorbent is made by trial-and-error, requiring expensive and
4 time-consuming experimental measurements of adsorption equilibrium. A much more
5 efficient alternative would be to choose the desorbent based on computational
6 simulations of the SMB process, minimizing the need for experiments. However, this
7 requires a simulation approach that can accurately predict multi-component adsorption
8 equilibrium in the adsorbent material, and then feed this data into a large-scale
9 simulation of the process – in other words, a simulation approach that goes from
10 molecules to processes.
11
12

13
14
15
16
17
18
19
20
21 In this study, we attempt to achieve this goal by combining molecular simulation of
22 adsorption with process simulations. Single component adsorption isotherms of all the
23 four species herein studied, as well as binary mixtures of ethane/ethylene,
24 ethane/propane, ethylene/propane, ethane/*n*-butane, and ethylene/*n*-butane in zeolite
25 13X were calculated by the configurational-bias Monte Carlo (CBMC) technique.
26
27
28
29
30
31
32
33
34
35
36
37
38
39
40
41
42
43
44
45
46
47
48
49
50
51
52
53
54
55
56
57
58
59
60
Molecular simulations are the first prediction tool to be used here, aiming to replace
expensive, time consuming and, in some cases, dangerous experiments. We adopted
force fields that have been widely used to predict adsorption of hydrocarbons in zeolites
(Calero *et al.*, 2004, Lamia *et al.*, 2009, Granato *et al.*, 2010), and use them to reproduce
experimental data on single component adsorption of ethane and ethylene in 13X
zeolite, as well as their binary mixtures with propane and *n*-butane. Subsequently, a
four-section Simulated Moving Bed (SMB) unit is analyzed through simulation, in
order to describe the behaviour of the unit by means of a mathematical model. This
model makes use of the equilibrium adsorption data, predicted by molecular simulation,
in a wide range of operating conditions. We demonstrate that this integrated approach is
a powerful tool for computational design of adsorptive separation processes.

2. Computational Details

2.1 – Molecular Simulation Methods

The configurational-bias Monte Carlo (CBMC) technique in the grand-canonical (μVT) ensemble has been extensively applied for calculation of adsorption properties, such as isotherms and heats of sorption. This technique allows for accurate calculations of the adsorbed amount, since it allows the total number of molecules to vary by way of creation and deletion Monte Carlo trials. A detailed explanation of this simulation technique can be found elsewhere (Vlugt *et al.*, 1999; Smit and Krishna, 2001; Frenkel and Smit, 2002). For simple hydrocarbons, such as alkanes or alkenes, a number of 2×10^6 cycles is enough to reach equilibrium. The United Atom (UA) force field was chosen to model the adsorbates due to a good compromise between accuracy and computational effort, when compared to the All Atom (AA) or the Anisotropic United Atom (AUA) force fields. These models are widely described in the literature (Martin and Siepmann, 1998; Ungerer *et al.*, 2000). For calculations of adsorption properties, such as isotherms and heats of sorption, the UA model is advantageous because of its reduced set of parameters to represent the inter- and intra-molecular interactions between the pseudo-atoms.

The 13X zeolite framework model is the sodium form of the Faujasite (FAU) type zeolite, obtained by randomly replacing silicon by aluminium, satisfying the Löwenstein rule. This substitution generates a negatively charged framework which is compensated by inserting 88 sodium cations, yielding a composition of $\text{Na}_{88}\text{Al}_{88}\text{Si}_{104}\text{O}_{384}$ per unit cell. The cations are allowed to move inside the zeolite. Periodic boundary conditions were applied in all directions. A rigid structure was

considered for the zeolite, since framework flexibility has little influence on adsorption properties in zeolites (Vlugt and Schenk, 2002).

Non-bonded interactions are described by Lennard-Jones potentials, as shown in Equation 1. A truncated and shifted potential is applied ($r_{cut} = 12 \text{ \AA}$), and tail corrections are not used (Dubbeldam *et al.*, 2004). Electrostatic interactions are calculated by the Ewald summation which is largely described elsewhere (Frenkel and Smit, 2002; Martin and Siepmann, 1998).

$$U(r_{ij}) = \begin{cases} 4\varepsilon_{ij} \left[\left(\frac{\sigma_{ij}}{r_{ij}} \right)^{12} - \left(\frac{\sigma_{ij}}{r_{ij}} \right)^6 \right] & r_{ij} \leq r_{cut} \\ 0 & r_{ij} > r_{cut} \end{cases} \quad (1)$$

Equation 2 describes the Lorentz-Berthelot mixing rules, used to calculate the cross interactions between different united atoms, except for the interactions with the non-framework cations, which requires specific parameters (Vlugt, 2000).

$$\sigma_{ij} = \frac{1}{2}(\sigma_{ii} + \sigma_{jj}), \quad \varepsilon_{ij} = \sqrt{\varepsilon_{ii}\varepsilon_{jj}} \quad (2)$$

All adsorbate molecules were considered to be flexible, with intramolecular parameters taken from the TraPPE force-field (Martin and Siepmann, 1998). Parameters for the interactions between adsorbates and the framework were taken from our previous modelling work of propane/propylene adsorption on zeolite 13X (Granato *et al.*, 2007), which consisted of a modification of the original model by Calero *et al.* (2004). All molecular interaction parameters are given in Tables S1 and S2 of the Supporting Information File.

2.2 – SMB Process Simulations

Detailed descriptions of the gas phase SMB operation, the mathematical models, and required parameters can be found in the literature (Cheng and Wilson, 2001; Minceva *et al.*, 2003; Leão and Rodrigues, 2004; Sá Gomes *et al.*, 2008, 2009; Lamia *et al.*, 2009). In this study, a “classical” SMB mode of operation, making use of a desorbent species, as patented by Rodrigues *et al.* (2006), was chosen for the separation of a mixture of ethane–ethylene over 13X zeolite. In the mathematical model of the four-section SMB unit, a multicomponent extension of the Toth isotherm and a linear driving force (LDF) for the intra-particle mass transfer are assumed. The mathematical model further assumes plug flow with axial dispersion, no radial gradients inside the column, bed void fraction, radius and porosity of the particles are constant along the axial coordinate, negligible thermal effects, negligible pressure drop and fast rate of adsorption. The isothermal assumption for gas-phase SMB was tested by Sá Gomes *et al.* (2009) in the study of propane/propylene separation, and a temperature gradient of 4K was observed along the entire unit. More details can be found elsewhere (Cruz *et al.*, 2005; Minceva *et al.*, 2003; Leão and Rodrigues, 2004). The simulation of an SMB unit may be performed by two methods: the True Moving Bed (TMB), and the SMB approach. Both TMB and SMB model predictions of steady-state performance of the SMB unit are very close. So, the TMB model was selected to study the feasibility of this separation at different temperatures, and using the proposed desorbents – propane and *n*-butane. The Separation Volume methodology (Azevedo and Rodrigues, 1999) was used to find the operating conditions of the SMB unit.

3. Results and Discussion

3.1. Ethane, Ethylene, Propane and *n*-Butane Single Component Adsorption in Zeolite 13X

Single component isotherms of ethane and ethylene adsorption in zeolite 13X were simulated at temperatures of 305, 393 and 423 K, and pressure ranges from 1 to 200 kPa. There are many experimental studies on adsorption of ethane and ethylene over Na-Faujasites in the literature (Danner and Choi, 1978; Kaul, 1987; Dunne *et al.* 1996; Valezuela and Myers, 1989). Danner and Choi (1978) evaluated prediction models of adsorption equilibria of binary mixtures of ethane/ethylene on 13X pellets containing 20% by weight of inert clay binder and 80% percent synthetic zeolite; Dunne and co-workers made simultaneous measurements of isosteric heats of adsorption and adsorption isotherms of a series of gases, including C₂H₆, on adsorbents of varying pore structure and ion type (NaX, H-ZSM-5, Na-ZSM-5).

Figures 1 (a) and (b) show equilibrium adsorption isotherms of ethane and ethylene over zeolite 13X compared with experimental results. The shape of the isotherms is well reproduced, and there is good agreement between simulation results and the experimental data for pure gases. The slight differences between our simulations and experiments from Kaul (1987) are probably due to the use in experiments of pelletized zeolite that can present structural imperfections, pore blocking, surface adsorption, and inactivation of part of the zeolite. On the contrary, the simulations assume a perfect zeolite crystal, which can cause some differences between simulation results and experimental data. So, we also performed simulations of ethane at 305 K for comparison with experiments carried out with a commercial sample of NaX powder

(Dunne *et al.* 1996). Figure 2 shows an excellent agreement between simulations and experiments.

Equilibrium adsorption isotherms of propane and *n*-butane in zeolite 13X are equally well reproduced by our model, as shown in previous work (Granato *et al.*, 2007, 2010). For completeness, the comparison between experiment and simulation for propane and *n*-butane are given in the Supporting Information. It should be noted that the ethane/ethylene data were verified with experimental measurements up to 200 kPa, while *n*-butane/propane has been validated with experimental data measured up to ~110 kPa.

3.2. Adsorption of Binary Mixtures in Zeolite 13X

The good agreement obtained for pure-component adsorption gives us confidence to use our simulations for multi-component adsorption predictions. Nevertheless, we further validate our models by simulating binary adsorption equilibrium and comparing to results estimated from experimental single-component data using the multicomponent extended Toth model (Valezuela and Myers, 1989). The experimental single component adsorption equilibrium data for ethane and ethylene on 13X presented by Danner and Choi (1978) at 298K and 323K were fit with the Toth equation, described by equation 3:

$$q_i = q_{s,i} \frac{b_i P_i}{\left(1 + (b_i P_i)^{t_i}\right)^{1/t_i}} \quad (3)$$

where q_i represents the concentration of component i in the adsorbed phase, q_s is the saturation capacity, P_i is the partial pressure of component i , t_i is a parameter of the model that characterizes the system heterogeneity and b is the affinity constant that depends on the temperature, T , as follows:

$$b_i = b_{0,i} e^{\frac{-\Delta H_i}{RT}}, \quad (4)$$

where b_0 is the affinity constant at infinite temperature, ΔH is the isosteric heat of adsorption at zero loading and R is the universal gas constant. The parameters of the fit obtained are presented in Table 1. This table also presents the parameters of the Toth equation for propane taken from Da Silva and Rodrigues (1999), and the parameters for n -butane obtained from a fit to the experimental data presented by Tarek *et al.* (1995).

Da Silva and Rodrigues (1999) determined the adsorption isotherm data of propane from 303 to 473 K and up to 110 kPa. Tarek *et al.* (1995) determined the adsorption isotherm data of n -butane from 300 to 360K and up to 150 Torr (~20 kPa). The temperatures used in the SMB simulations are within the range studied by these authors. The maximum pressure used in the adsorption measurements for n -butane was high enough to obtain the saturation capacity. Da Silva and Rodrigues used pellets of 13X while Tarek *et al.* (1995) used powder. In a real unit, a shaped 13X would have to be used to avoid large pressure drops. Therefore the saturation capacity presented by Tarek *et al.* (1995) was reduced by 20% to represent the mass fraction of binder and to level with the data presented by Da Silva and Rodrigues (1999) and by Danner and Choi (1978) for ethane and ethylene.

The multicomponent extension of the Toth equation is described by:

$$q_i = q_{s,i} \frac{b_i P_i}{\left(1 + \left(\sum_{j=1}^{nc} b_j P_j\right)^{t_i}\right)^{1/t_i}} \quad (5)$$

The prediction of the multicomponent adsorption equilibrium obtained with this fit was compared with the binary data obtained by CBMC simulations. Excellent agreement was observed for all conditions tested. As an example, the comparison for ethane/ethylene binary adsorption equilibrium data at 323K and a total pressure of 137.8

1
2
3 kPa is presented in Figure 3. Results from binary adsorption experiments reported by
4
5 Kaul (1987) are also included in this figure, and remarkable agreement between
6
7 simulation and experiment is observed.
8

9
10 Additional CBMC simulations for the binary adsorption equilibria of propane and
11
12 *n*-butane with ethane and ethylene, respectively, have been carried out at 373 K and
13
14 several molar fractions. The simulation results are compared with data provided by the
15
16 extended Toth model (Valezuela and Myers, 1989) for propane/ethane,
17
18 propane/ethylene, *n*-butane/ethane, and *n*-butane/ethylene systems, using the data from
19
20 pure component adsorption isotherms. The resulting x-y diagrams are shown in Figures
21
22 4a and 4b. The set of force field parameters successfully reproduce the equilibrium
23
24 adsorption properties of the binary mixtures propane and *n*-butane with ethylene and
25
26 ethane.
27
28

3.3 - Simulated Moving Bed Simulations

29
30
31
32 The next step in our multiscale modelling strategy is to use molecular simulation data,
33
34 presented in the previous sections, directly as input into the SMB model. The separation
35
36 regions of the gas phase simulating moving bed (SMB) were obtained by simulation and
37
38 are presented in Figures 5 and 6. The gammas represent the ratio between the fluid
39
40 velocity, v_j , in the respective section and the solid velocity, u_s , as described by
41
42
43

$$\gamma_j = \frac{v_j}{u_s} \quad (5)$$

44
45
46
47 where j is the SMB section (I, II, III, IV).
48

49
50 Table 2 presents the model parameters chosen to obtain the separation region. The
51
52 properties of the adsorbent were taken from Da Silva and Rodrigues (1999). It should be
53
54 noted that the separation region does not depend on the values of gamma 1 and gamma
55
56 4 as long as they are large enough and small enough, respectively, to ensure that
57
58
59
60

1
2
3 sections I and IV are cleaned. Furthermore, the advantage of representing the separation
4 region in terms of the dimensionless variables γ_2 and γ_3 is that these
5 results do not depend on the size of the columns (unless there is a strong mass transfer
6 resistance, which is not the case here). This means that a point can be chosen from the
7 separation region and we can either obtain the size of a unit for a given feed flow rate or
8 obtain the feed flow rate for a given size.
9
10
11
12
13
14
15

16 Figure 7 shows the adsorption capacity of the four species at 298, 323, 373 and 423
17 K, obtained from the parameters presented in Table 1. Propane has an intermediate
18 adsorption capacity, which is a desired property for a desorbent in a simulated moving
19 bed process. Ethylene is the species with the highest adsorption capacity; therefore, a
20 mixture of ethylene and propane will be obtained in the extract of the SMB. Ethane, as
21 the least adsorbed species, will be obtained in the raffinate together with propane.
22 However, *n*-butane has a strong interaction with the adsorbent, which means that it will
23 hardly be displaced by the other species. It has a lower saturation capacity (crosses the
24 other isotherms at a pressure below 100 kPa) which, depending on the temperature and
25 feed composition, may not be able to displace the other two adsorbates.
26
27
28
29
30
31
32
33
34
35
36
37

38 It is worth mentioning that at 323 K the equilibrium adsorption isotherm of propane is
39 between the ones of ethane and ethylene while at 373 K, the propane isotherm crosses
40 the ethylene adsorption isotherm at around 40 kPa.
41
42
43
44

45 The separation region for a feed of 80% ethylene and 20% ethane at 110 kPa and 298,
46 323, 348 and 373 K, using 13X as adsorbent and propane as desorbent, and a switching
47 time of 76.5s is presented in Figure 5. The separation region for the case where *n*-butane
48 is used as desorbent is presented in Figure 6. These regions represent the production of
49 both ethane and ethylene with purities above 99.5%. As mentioned by Gleich (US
50 Patent 3921411 - 1975), the composition of the feed of a C2-splitter can widely change
51
52
53
54
55
56
57
58
59
60

1
2
3 upon the choice of the feedstock and of the sequence selected upstream the splitter.
4
5 Typical feed compositions have an ethane/ethylene ratio from about 1:3 to 3:1. The feed
6
7 composition chosen in this work is similar to the one presented in Example II of that
8
9 patent.
10

11
12 As it can be seen from the simulation results, the separation is feasible. When propane
13
14 is used as desorbent it can be clearly observed that the separation region increases with
15
16 the decrease of the temperature. This is due to the increase of the adsorption capacity (as
17
18 shown in Figure 7), and to the increase of the selectivity. Figure 8 presents the
19
20 adsorption capacity of different mixtures of ethane/ethylene at a total pressure of 110
21
22 kPa and at 323 and 373 K obtained from the parameters presented in Table 1 and with
23
24 Equation 5. As it can be seen, the increase of the temperature decreases the selectivity
25
26 of the adsorbent towards each species. As mentioned before, this decrease of the
27
28 selectivity decreases the separation region. When *n*-butane is used as desorbent this
29
30 effect of the selectivity in the separation region is not so clear. This is due to the strong
31
32 interaction of *n*-butane with the adsorbent, which makes it hard to be displaced by
33
34 ethane and by ethylene.
35
36
37

38
39 Additionally, the heights of the “triangle” that represents the separation region are
40
41 much smaller when *n*-butane is used. This indicates a smaller productivity when using
42
43 this desorbent. The dimensionless velocity in zone IV, however, is much smaller when
44
45 *n*-butane is used. For the same time switch this is translated in a lower flow rate of the
46
47 recycle pump and thus, in a smaller energy consumption of the SMB unit. However, the
48
49 overall energy consumption, i.e., the energy consumption of the SMB and the energy
50
51 consumption of the units to separate ethane and ethylene from the desorbent, rather than
52
53 the energy consumption of the SMB unit alone, is the one that must be taken into
54
55 account.
56
57
58
59
60

1
2
3 Although the separation region at 298 K when using propane as desorbent is the
4 largest, from an industrial point of view, the operation at 323 K is more favourable.
5 Additionally, economical aspects should be taken into consideration for selecting the
6 best operating temperature. At 298 K the adsorption isotherms of ethane and ethylene
7 are very steep (see Figure 7). As a consequence, the desorbent consumption will be
8 equally large.
9

10
11 An operation point was selected in the separation region (black dot in Figures 5 and
12 6), at 323 K. The operating conditions of these points are presented in Table 3. The
13 concentration profiles along the unit for the chosen operation point are presented in
14 Figure 9, for propane as desorbent and in Figure 10, for *n*-butane as desorbent. The
15 performance parameters of the unit, i.e., purity (Pur) of the streams, and recovery (Rec),
16 are all 100%. The desorbent consumption (DC) is 0,803 m³ of propane / kg of ethylene
17 in the extract, and 0,798 m³ of *n*-butane / kg of ethylene in the extract. Productivity
18 (Prod) of ethylene is 3.64 mol.kg⁽⁻¹⁾.h⁽⁻¹⁾, using propane as desorbent. On the other hand,
19 when *n*-butane is used as desorbent, the calculated productivity of ethylene is 0.20
20 mol.kg⁽⁻¹⁾.h⁽⁻¹⁾. As it can be seen, at these operating conditions, a large productivity may
21 potentially be obtained for ethane/ethylene separation by SMB using 13X as adsorbent
22 and propane as desorbent. As expected from the separation regions, the productivity
23 when *n*-butane is used as desorbent is much lower.
24
25

26
27 For these operating points, if we consider a feed flow rate of 1.35 m³/s, we need
28 columns with 7.71 m³, when using propane as desorbent, and columns with 140.30 m³,
29 when using *n*-butane as desorbent. For propane as desorbent the extract flow rate would
30 be 1.77 m³/s, the raffinate flow rate 1.83 m³/s, and the desorbent flow rate 2.25 m³/s.
31 For *n*-butane as desorbent the extract flow rate would be 2.03 m³/s, the raffinate flow
32 rate 1.88 m³/s, and the desorbent flow rate 2.56 m³/s.
33
34
35
36
37
38
39
40
41
42
43
44
45
46
47
48
49
50
51
52
53
54
55
56
57
58
59
60

4. Conclusions

In this paper we present a multiscale *in silico* strategy to design an SMB separation unit that combines molecular simulation with process modelling, and applied it to the challenging separation of ethane and ethylene using zeolite 13X. The molecular model was validated first by comparing simulated single-component adsorption isotherms for ethane and ethylene on 13X with experimental data from several literature sources, and subsequently by comparing binary Monte Carlo simulations to estimates from the extended Toth model based on experimental single-component data. In all cases studied, there was very good agreement between simulation and experiment, giving us confidence to use our model as an adsorption prediction tool.

The results from molecular simulation were then directly used as input to the process simulation of an SMB unit to accomplish the separation of ethane and ethylene. Two candidate desorbents were evaluated, namely propane and *n*-butane. Overall, propane was found to be the most advantageous of the two candidates for this particular separation. Our results thus show that the complete separation of an ethane/ethylene mixture is feasible by SMB with a large productivity, using 13X as adsorbent and propane as desorbent. At this stage, we have not attempted to optimize the SMB unit, but it is likely that doing so will lead to even better separation performance.

The strategy presented here gives a good understanding on how molecular simulations can be coupled with a model for industrial applications. The results obtained from well established techniques provide a solid tool for an integrated approach from the molecular scale to process design. The choice of a good system sorbent/desorbent can be made more efficient by applying simulation techniques, provided there is an adequate combination of knowledge of these two scientific fields: molecules and processes.

5. Nomenclature

b	Affinity constant that depends on the temperature.
D_{ax}	Axial dispersion.
ΔH	Heat of adsorption.
k_s	Intraparticle mass transfer coefficient in the LDF model.
$k_{1,2}$	Constants related to the bonded interactions: bond stretching and bond bending, respectively.
q	In Table S1, refers to the partial charges of the cations and framework atoms.
q_i	Adsorbed phase concentration.
q_{max}	Maximum adsorbed phase concentration.
r	Bond length.
r_{cut}	Cut-off radius.
P, P_i	Pressure, partial pressure of component i .
T	Absolute temperature.
t_i	System heterogeneity parameter
t^*	Switching time.
u_s	Solid velocity
$U_{(r)}$	Van der Waals potential energy
V	Volume.
Greek letters	
ε	Characteristic energy in pair potential.
ε_b	Particle porosity.
γ	The ratio between the fluid velocity, v_j , in the respective section and the solid velocity, u_s , where j is the SMB section.

1		
2		
3		
4	ϕ	Torsion angle.
5		
6	v_j	Fluid velocity.
7		
8	η	Constants related to torsional configurations.
9		
10		
11	μ	Chemical potential.
12		
13	ρ	Particle density.
14		
15	θ	Bending angle.
16		
17		
18	σ	Characteristic distance in pair potential.
19		
20		
21		
22		
23		
24		
25		
26		
27		
28		
29		
30		
31		
32		
33		
34		
35		
36		
37		
38		
39		
40		
41		
42		
43		
44		
45		
46		
47		
48		
49		
50		
51		
52		
53		
54		
55		
56		
57		
58		
59		
60		

Acknowledgements

MAG thanks financial support from Fundação para a Ciência e a Tecnologia (FCT) under the post-doctoral grant SFRH-BPD-47432-2008. VMS acknowledges a scholarship from project PTDC-EQU-ERQ-104413-2008. This work is partially supported by projects PTDC-EQU-ERQ-104413-2008 and PEst-C/EQB/LA0020/2011, financed by FEDER through COMPETE - Programa Operacional Factores de Competitividade and by FCT - Fundação para a Ciência e a Tecnologia.

Literature Cited

Azevedo, D. C. S.; Rodrigues, A. E. "Design of a Simulated Moving Bed in the Presence of Mass Transfer Resistance," *AIChE Journal*. **45**, 956-966, (1999).

Calero, S.; Dubbeldam, D.; Krishna, R.; Smit, B.; Vlugt, T. J. H.; Denayer, J. F. M.; Martens, J. A.; Maesen, T. L. M. "Understanding the Role of Sodium During Adsorption: A Force Field for Alkanes in sodium-Exchanged Faujasites," *J. Am. Chem. Soc.*, *126*, 11377-11386 (2004).

Cheng, L. S. and S. T. Wilson, "Process for separating propylene from propane," US Patent 6,293,999 (2001).

Cruz, P.; Santos, J. C.; Magalhães, F. D.; Mendes, A. "Simulation of Separation Processes Using Finite Volume Method," *Computers & Chemical Engineering*, **30**, 83-98, (2005).

Da Silva, F.A.; Rodrigues, A. E. "Adsorption Equilibria and Kinetics for Propylene and Propane Over 13X and 4A Zeolite Pellets," *Ind. Eng. Chem. Res.*, **38**, 2434-2438 (1999).

1
2
3 **Danner, R. P.; Choi, E. C. F.** “Mixture Adsorption Equilibria of Ethane and
4 Ethylene on 13X Molecular Sieves,” *Ind. Eng. Chem. Fundam.* **17**, 248-253 (1978).
5
6

7
8 **Dubbeldam, D.; Calero, S.; Vlugt, T. J. H.; Krishna, R.; Maesen, T. L. M.;**
9 **Smit, B.** “United Atom Force Field for Alkanes in Nanoporous Materials,” *J. Phys.*
10 *Chem. B.* **108**, 12301–12313, (2004).
11
12

13
14
15 **Dunne, J. A.; Rao, M.; Sircar, S.; Gorte, R. J.; Myers, A. L.** “Calorimetric Heats
16 of Adsorption and Adsorption Isotherms. 2. O₂, N₂, Ar, CO₂, CH₄, C₂H₆, and SF₆
17 on NaX, H-ZSM-5, and Na-ZSM-5 Zeolites,” *Langmuir*, **12**, 5896-5904 (1996).
18
19

20
21 **Frenkel, D.; Smit, B.** “Understanding Molecular Simulations: From Algorithms to
22 Applications,” 2nd ed.; *Academic Press*: San Diego, (2002).
23
24

25
26
27 **Gleich, W. A.** “C₂-Splitter Operation with Side Draw Removal of Water to Prevent
28 Hydrate Formation”. *US Patent* no. 3921411 (1975).
29
30

31
32
33 **Granato, M. A.; Lamia, N.; Vlugt, T. J. H.; Rodrigues, A. E.** “Adsorption
34 Equilibrium of Isobutane and 1-Butene in Zeolite 13X by Molecular Simulation,”
35 *Ind. Eng. Chem. Res.* **47**, 6166-6174, (2008).
36
37

38
39
40 **Granato, M. A.; Vlugt, T. J. H.; Rodrigues, A. E.** “Molecular Simulation of
41 Propane-Propylene Binary Adsorption Equilibrium in Zeolite 13X,” *Ind. Eng.*
42 *Chem. Res.* **46**, 7239-7245, (2007).
43
44

45
46
47
48 **Granato, Miguel A., Vlugt, Thijs J. H., Rodrigues, Alirio E.** “Potential
49 Desorbents for Propane/Propylene Separation by Gas Phase Simulated Moving Bed:
50 A Molecular Simulation Study,” *Ind. Eng. Chem. Res.*, **49**, 5826-5833 (2010).
51
52
53
54
55
56
57
58
59
60

1
2
3 **Kaul, B. K.** “A modern version of volumetric apparatus for measuring gas-solid
4 equilibrium data”. *Ind. Eng. Chem. Res.* **26**, 928-983 (1987).
5
6

7
8 **Kirk-Othmer**, “Encyclopedia of Chemical Technology” *Wiley*: New York, U.S.A.
9 1991.
10

11
12
13 **Lamia, N.; Granato, M. A.; Sá Gomes. P.; Grande, C. A.; Wolff, L.; Leflaive.**
14 **P.; Leinekugel-Le-Cocq, D.; Rodrigues, A. E.** “Propane/Propylene Separation by
15 Simulated Moving Bed II. Measurement and Prediction of Binary Adsorption
16 Equilibria of Propane, Propylene, Isobutane, and 1-Butene on 13X Zeolite,”
17 *Separation Science and Technology*, **44**, 1485-1509 (2009).
18
19

20
21
22 **Leão, C. P.; Rodrigues, A. E.** “Transient and Steady-State Models for Simulated
23 Moving Bed Processes: Numerical Solutions,” **Computers & Chemical**
24 **Engineering**, **28** (9), 1725-1741 (2004).
25
26

27
28
29 **Martin, M. G.; Siepmann, J. I.** “Transferable Potentials for Phase Equilibria – 1:
30 United-Atom Description of *n*-Alkanes,” *J. Phys. Chem. B*, **102**, 2569–2577, (1998).
31
32

33
34
35 **Mazzotti, M.; Baciocchi, R.; Storti, G.; Morbidelli, M.** “Vapor-Phase SMB
36 Adsorptive Separation of Linear/Nonlinear Paraffins,” *Ind. Eng. Chem. Res.*, **35**,
37 2313-2321 (1996).
38
39

40
41
42 **Minceva, M.; Pais, L. S.; Rodrigues, A. E.** “Cyclic Steady State of Simulated
43 Moving Bed Processes for Enantiomers Separation,” *Chemical Engineering and*
44 *Processing*, **42**, 93-104 (2003).
45
46

47
48
49 **Rao, D. P.; Sivakumar, S. V.; Mandal, S.; Kota, S.; Ramaprasad, B.S.G.** “Novel
50 simulated moving-bed adsorber for the fractionation of gas mixtures,” *J.*
51 *Chromatogr. A.*, **1069**, 141–151, (2005).
52
53
54
55
56
57
58
59
60

1
2
3 **Rege, S. U.; Padin, J.; Yang, R. T.** “Olefin/Paraffin Separations by Adsorption: π -
4 Complexation vs. Kinetic Separation,” *AIChE Journal*, **44**, 799-809 (1998).
5
6

7
8 **Rodrigues, A. E.; Lamia, N.; Grande, C.; Wolff, L.; Leflaive, P.; Leinekugel-le-**
9 **Cocq, D.** “Procédé de Séparation du Propylène en Mélange avec du Propane par
10 Adsorption en Lit Mobile Simulé en Phase Gaz ou Liquide Utilisant une Zéolithe de
11 type Faujasite 13X comme Solide Adsorbant”. *FR. Patent* no. 2903981A1 and *INT.*
12 *Patent* WO/2008/012410A1. (2006). Also: *US. Patent* no. 20100069696. (2010).
13
14
15
16
17

18
19
20 **Sá Gomes, P.; Minceva, M.; Rodrigues, A. E.** “Operation of an Industrial SMB
21 Unit for p-xylene Separation Accounting for Adsorbent Ageing Problems,”
22 *Separation Science and Technology*, **43**, 1974-2002 (2008).
23
24
25

26
27 **Sá Gomes, P.; Lamia, N.; Rodrigues, A. E.** “Design of a gas-phase simulated
28 moving bed for propane/propylene separation” *Chemical Engineering Science*, **64**,
29 1336-1357 (2009).
30
31
32

33
34
35 **Smit, B.; Krishna, R.** “Monte Carlo Simulations in Zeolites,” *Curr. Opin. Solid*
36 *State Mater. Sci.*, **5**, 455-461, (2001).
37
38

39
40 **Tarek, M.; Kahn, R.; de Lara, E. C.** “Modelization of Experimental Isotherms of
41 n-Alkanes in NaX Zeolite,” *Zeolites*, **15**, 67-72, (1995).
42
43
44

45
46 **Ungerer, P.; Beauvais, C.; Delhommelle, J.; Boutin, A.; Rousseau, B.; Fuchs. A.**
47 **H.** “Optimization of the Anisotropic United Atoms Intermolecular Potential for n-
48 Alkanes,” *J. Chem. Phys.*, **112**, 5499-5510, (2000).
49
50

51
52
53 **Valenzuela, D. P.; Myers, A. L.** “Adsorption Equilibrium Data Handbook, p. 89-
54 90. *Prentice-Hall*, Engelwood Cliffs, N.J. (1989).
55
56
57
58
59
60

1
2
3 **Vlugt, T. J. H.; Krishna R.; Smit, B.** Molecular Simulations of Adsorption
4
5 Isotherms for Linear and Branched Alkanes and Their Mixtures in Silicalite. *J.*
6
7 *Phys. Chem. B.* **103**, 1102-1118, (1999).
8
9

10 **Vlugt, T. J. H.; Schenk M:** Influence of Framework Flexibility on the Adsorption
11
12 Properties of Hydrocarbons in the Zeolite Silicalite. *J. Phys. Chem. B.*, **106**, 12757-
13
14 12763, (2002).
15
16
17
18
19
20
21
22
23
24
25
26
27
28
29
30
31
32
33
34
35
36
37
38
39
40
41
42
43
44
45
46
47
48
49
50
51
52
53
54
55
56
57
58
59
60

For Peer Review

Table 1 - Parameters of the Toth Equation.

Parameter	Ethane	Ethylene	Propane ^a	n-Butane ^b
q_s [mol/kg]	2.21	2.72	2.68	1.57
b_0 [kPa ⁻¹ l]	5.22×10^{-6}	1.13×10^{-7}	3.50×10^{-7}	1.37×10^{-6}
$-\Delta H$ [kJ/mol]	21.4	36.3	35.8	41.2
t [-]	1.75	0.97	0.58	0.94

^a Data from da Silva (1999)²⁵.

^b Data from Tarek et al (1995)²⁶.

Table 2 – SMB Model Parameters.

Parameter	Value	Units	
D_{ax}	3.76×10^{-4}	m^2/s	
ε_b	0.4	-	
ρ_p	1357	kg/m^3	
$k_{s,i}$	1	s^{-1}	
T	323	K	
P	110	kPa	
t^*	76.5	s	
	Propane	<i>n</i> -Butane	
γ_I	100	150	-
γ_{IV}	0.05	0.01	-
Feed Composition (molar fraction)		Units	
Ethylene	0.8	-	
Ethane	0.2	-	
Configuration	2-2-2-2	-	

Table 3 – Operating Conditions of the Selected Point for the unit using Propane and n-Butane as desorbents.

Parameter	Propane	n-Butane	Units
t^*	76.5	76.5	s
γ_I	80	4	-
γ_{II}	21	0.85	-
γ_{III}	66	2.95	-
γ_{IV}	5	0.02	-

List of Figures

Figure 1 – Isotherms on 13X zeolite at 393 and 423 K: (a) Ethane; (b) Ethylene. Open symbols are experimental data from Kaul, (1987). Closed symbols are our simulations, which account for the presence of 20% of binder in the experimental sample.

Figure 2 – Isotherms of Ethane on 13X zeolite at 305 K. Open symbols are experimental data from Dunne *et al.*, (1996). Closed symbols are our simulations.

Figure 3 – Binary adsorption equilibrium for ethane/ethylene at a total pressure of 137.8 kPa, calculated from the extended Toth model with experimental single component data from Danner and Choi (1978), predicted from CBMC simulations, and compared with experimental binary adsorption data from Kaul (1987).

Figure 4a – Binary adsorption equilibrium at 373 K and total pressure of 110 kPa. ^(a,b)Experimental single component data used in the extended Toth model were taken from Danner and Choi (1978) for ethane and ethylene, and from Tarek *et al.* (1995) for n-butane.

Figure 4b – Binary adsorption equilibrium at 373 K and total pressure of 110 kPa. ^(a,b)Experimental single component data used in the extended Toth model were taken from Danner and Choi (1978) for ethane and ethylene, and from Da Silva and Rodrigues (1999) for propane.

Figure 5 – Separation regions obtained by simulation using propane as desorbent at four different temperatures, and at P=110 kPa. The selected operating point is shown as a black circle.

Figure 6 – Separation regions obtained by simulation using n-butane as desorbent at four different temperatures, and at P=110 kPa. The selected operating point is shown as a black circle.

Figure 7 - Single component isotherms at different temperatures.

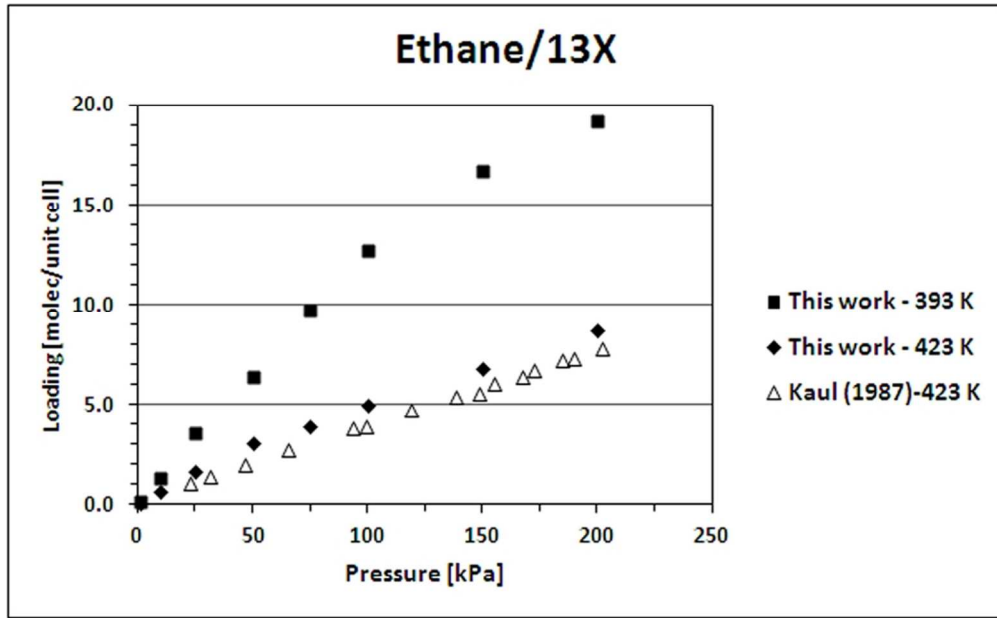
Figure 8 - Binary component equilibrium diagrams at different temperatures.

Figure 9 - Concentration profile along the unit for the selected operating point using propane as desorbent.

Figure 10 - Concentration profile along the unit for the selected operating point using n-butane as desorbent.

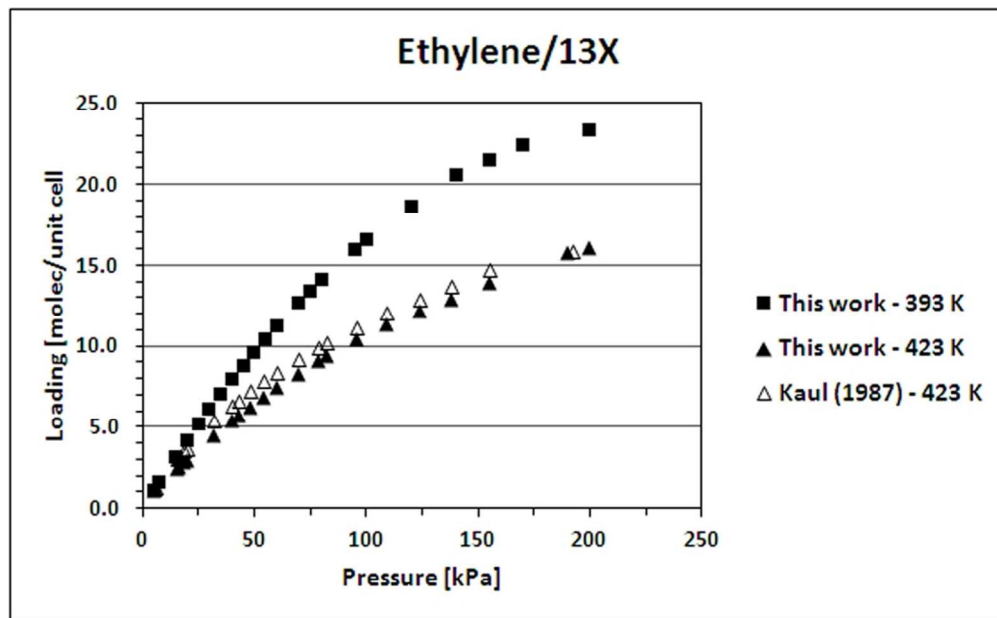
Figure S1 – Isotherms of propane and n-butane. Taken from Granato *et al.* (2007, 2010).

1
2
3
4
5
6
7
8
9
10
11
12
13
14
15
16
17
18
19
20
21
22
23
24
25
26
27
28
29
30
31
32
33
34
35
36
37
38
39
40
41
42
43
44
45
46
47
48
49
50
51
52
53
54
55
56
57
58
59
60



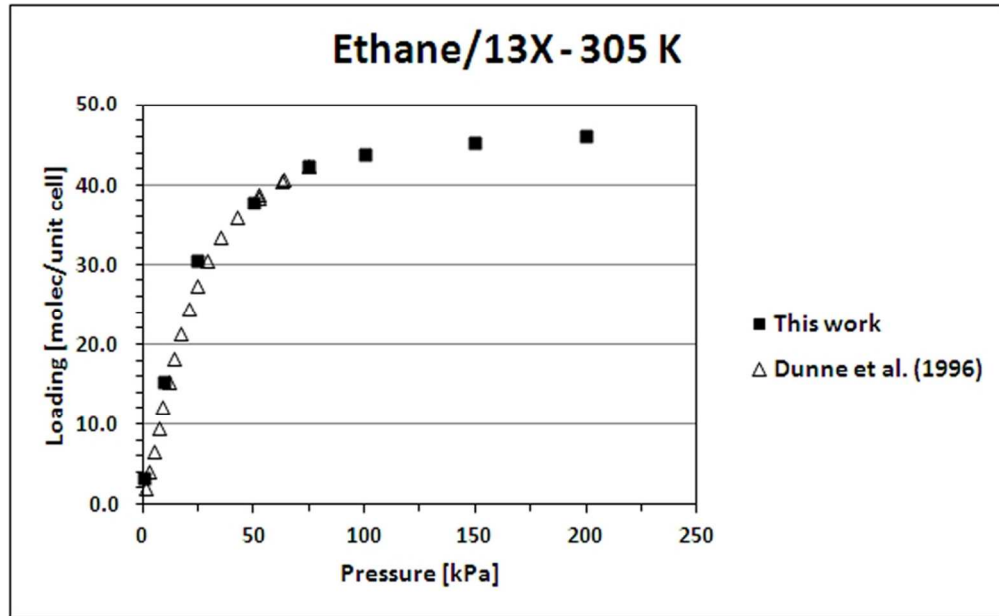
86x53mm (300 x 300 DPI)

Review



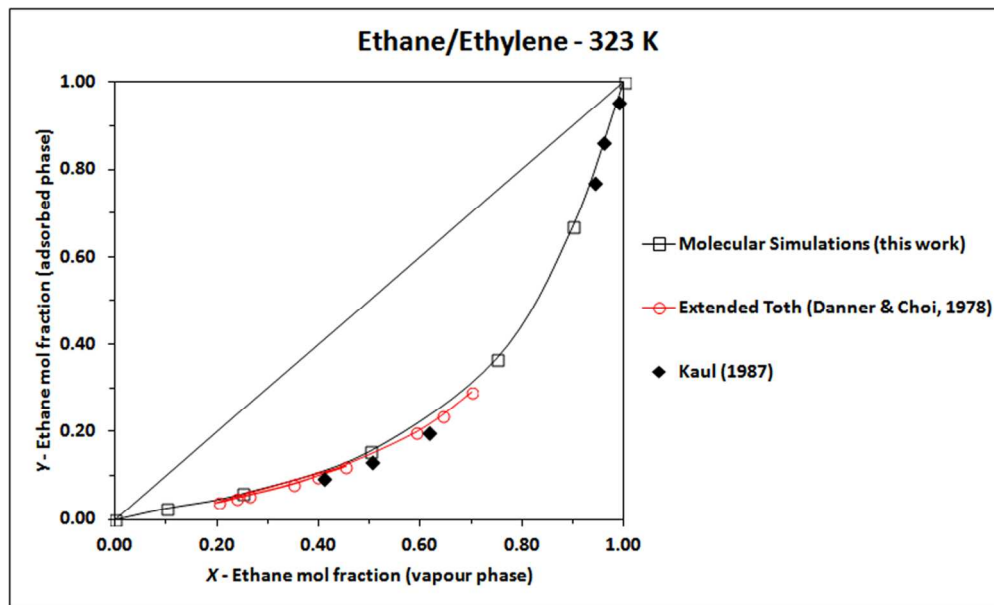
28 Figure 1 – Isotherms on 13X zeolite at 393 and 423 K: (a) Ethane; (b) Ethylene. Open symbols are
29 experimental data from Kaul, (1987). Closed symbols are our simulations, which account for the presence of
30 20% of binder in the experimental sample.
31 86x53mm (300 x 300 DPI)

1
2
3
4
5
6
7
8
9
10
11
12
13
14
15
16
17
18
19
20
21
22
23
24
25
26
27
28
29
30
31
32
33
34
35
36
37
38
39
40
41
42
43
44
45
46
47
48
49
50
51
52
53
54
55
56
57
58
59
60



28 Figure 2 – Isotherms of Ethane on 13X zeolite at 305 K. Open symbols are experimental data from Dunne et
29 al., (1996). Closed symbols are our simulations.
30 86x53mm (300 x 300 DPI)

31
32
33
34
35
36
37
38
39
40
41
42
43
44
45
46
47
48
49
50
51
52
53
54
55
56
57
58
59
60

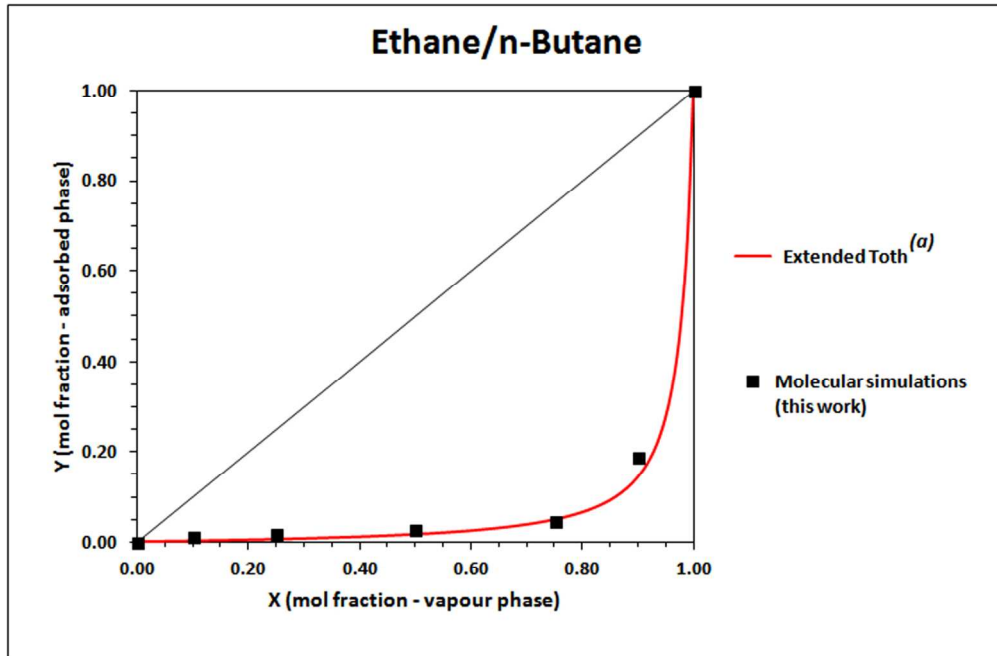


27
28
29
30
31
32
33
34
35
36
37
38
39
40
41
42
43
44
45
46
47
48
49
50
51
52
53
54
55
56
57
58
59
60

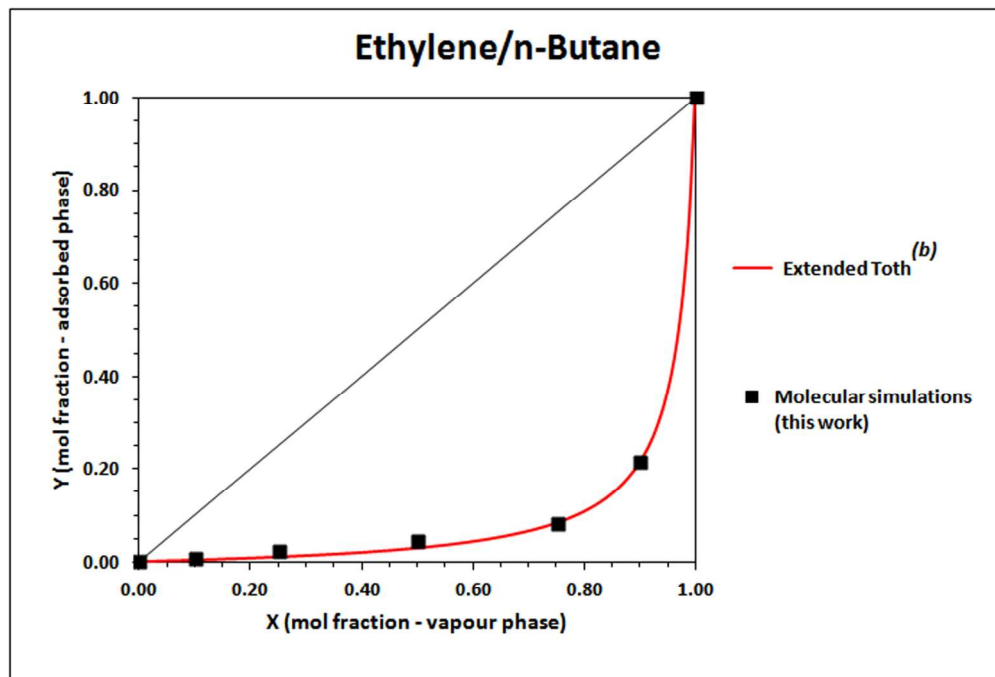
Figure 3 - Binary adsorption equilibrium for ethane/ethylene at a total pressure of 137.8 kPa, calculated from the extended Toth model with experimental single component data from Danner and Choi (1978), predicted from CBMC simulations, and compared with experimental binary adsorption data from Kaul (1987).

140x84mm (300 x 300 DPI)

1
2
3
4
5
6
7
8
9
10
11
12
13
14
15
16
17
18
19
20
21
22
23
24
25
26
27
28
29
30
31
32
33
34
35
36
37
38
39
40
41
42
43
44
45
46
47
48
49
50
51
52
53
54
55
56
57
58
59
60



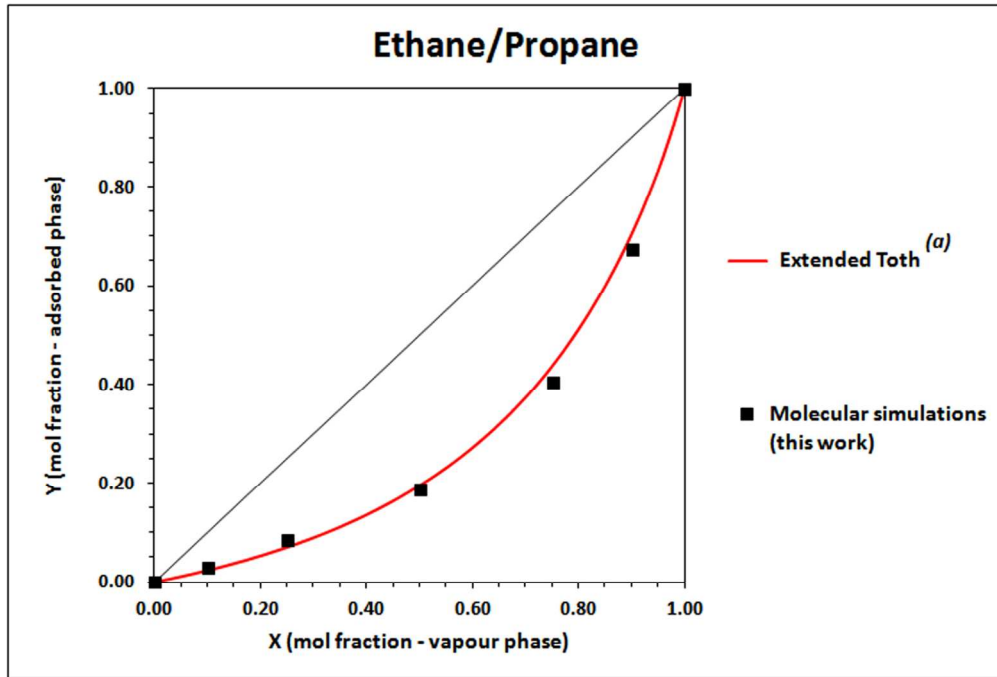
140x92mm (300 x 300 DPI)



30 Figure 4a - Binary adsorption equilibrium at 373 K and total pressure of 110 kPa. (a,b) Experimental single
31 component data used in the extended Toth model were taken from Danner and Choi (1978) for ethane and
32 ethylene, and from Tarek et al. (1995) for n-butane.
33 140x94mm (300 x 300 DPI)

34
35
36
37
38
39
40
41
42
43
44
45
46
47
48
49
50
51
52
53
54
55
56
57
58
59
60

1
2
3
4
5
6
7
8
9
10
11
12
13
14
15
16
17
18
19
20
21
22
23
24
25
26
27
28
29
30
31
32
33
34
35
36
37
38
39
40
41
42
43
44
45
46
47
48
49
50
51
52
53
54
55
56
57
58
59
60



140x94mm (300 x 300 DPI)

Review

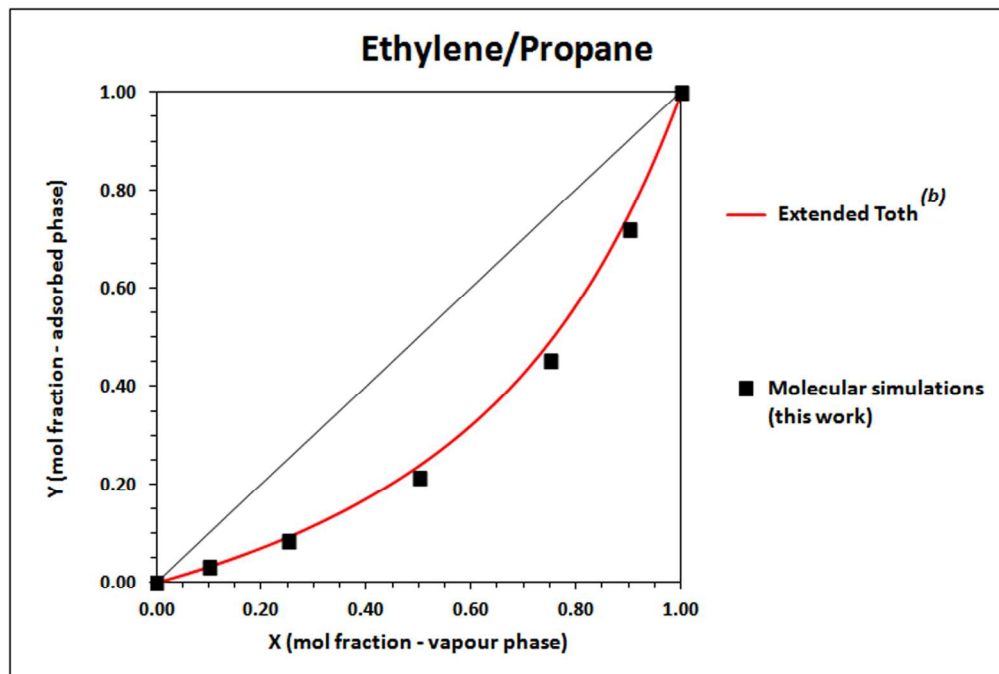
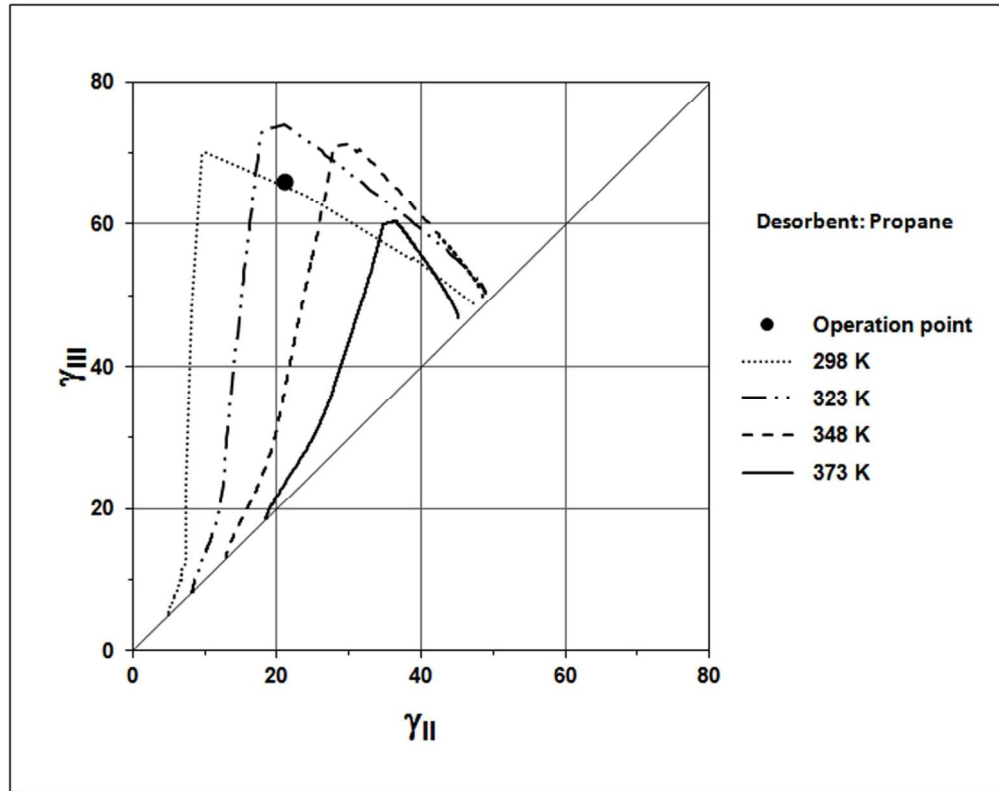


Figure 4b – Binary adsorption equilibrium at 373 K and total pressure of 110 kPa. (a,b) Experimental single component data used in the extended Toth model were taken from Danner and Choi (1978) for ethane and ethylene, and from Da Silva and Rodrigues (1999) for propane.
140x94mm (300 x 300 DPI)

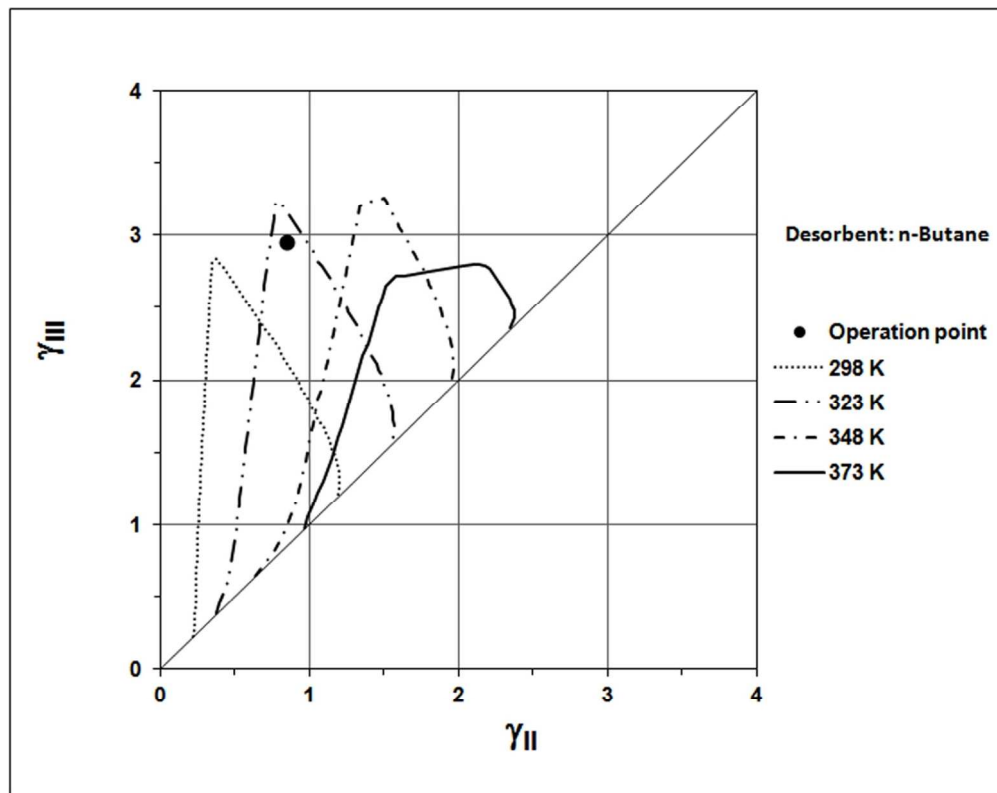


33
34
35
36

Figure 5 – Separation regions obtained by simulation using propane as desorbent at four different temperatures, and at $P=110$ kPa. The selected operating point is shown as a black circle.

37
38
39
40
41
42
43
44
45
46
47
48
49
50
51
52
53
54
55
56
57
58
59
60

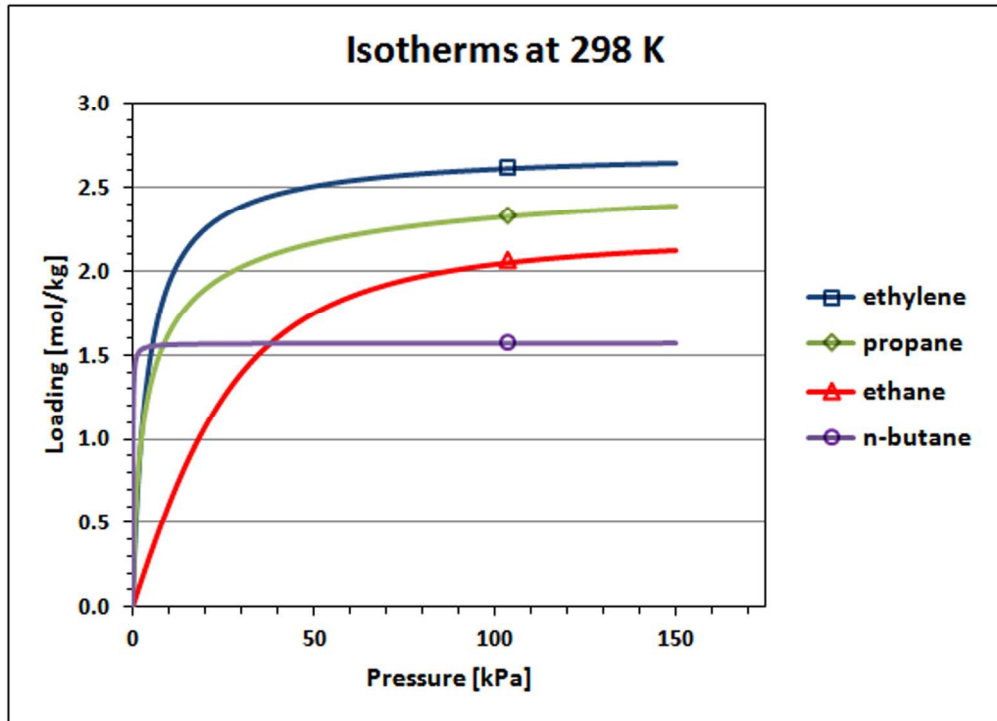
110x87mm (300 x 300 DPI)



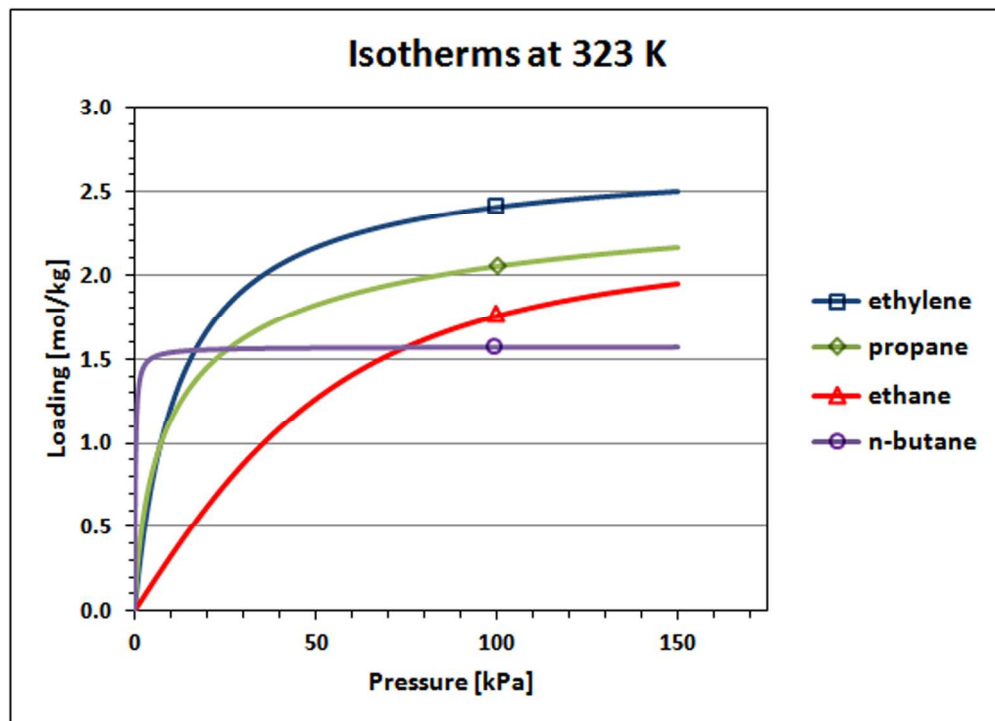
33
34
35
36
37
38
39
40
41
42
43
44
45
46
47
48
49
50
51
52
53
54
55
56
57
58
59
60

Figure 6 – Separation regions obtained by simulation using n-butane as desorbent at four different temperatures, and at P=110 kPa. The selected operating point is shown as a black circle.
110x87mm (300 x 300 DPI)

1
2
3
4
5
6
7
8
9
10
11
12
13
14
15
16
17
18
19
20
21
22
23
24
25
26
27
28
29
30
31
32
33
34
35
36
37
38
39
40
41
42
43
44
45
46
47
48
49
50
51
52
53
54
55
56
57
58
59
60

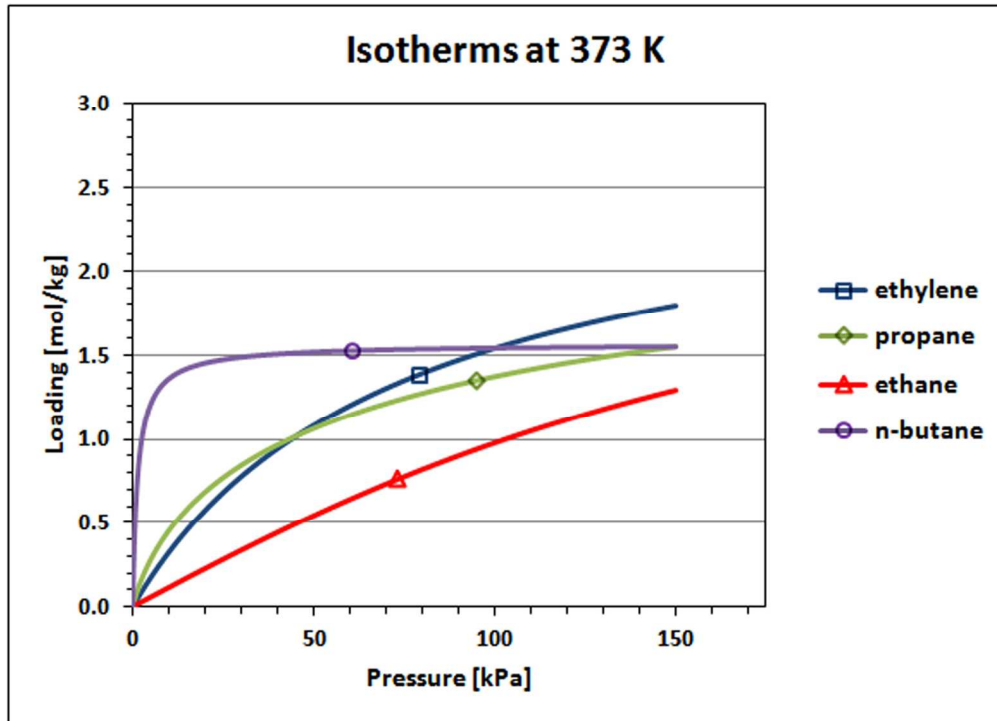


140x101mm (300 x 300 DPI)

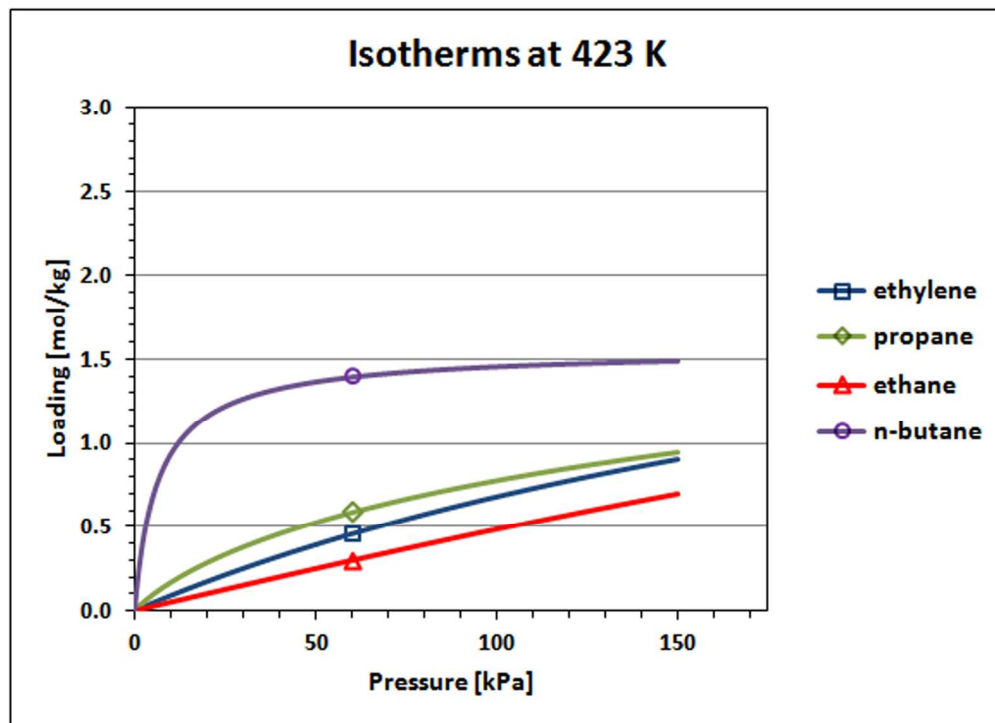


140x101mm (300 x 300 DPI)

1
2
3
4
5
6
7
8
9
10
11
12
13
14
15
16
17
18
19
20
21
22
23
24
25
26
27
28
29
30
31
32
33
34
35
36
37
38
39
40
41
42
43
44
45
46
47
48
49
50
51
52
53
54
55
56
57
58
59
60



140x101mm (300 x 300 DPI)



31
32
33
34
35
36
37
38
39
40
41
42
43
44
45
46
47
48
49
50
51
52
53
54
55
56
57
58
59
60

Figure 7 - Single component isotherms at different temperatures.
140x101mm (300 x 300 DPI)

1
2
3
4
5
6
7
8
9
10
11
12
13
14
15
16
17
18
19
20
21
22
23
24
25
26
27
28
29
30
31
32
33
34
35
36
37
38
39
40
41
42
43
44
45
46
47
48
49
50
51
52
53
54
55
56
57
58
59
60

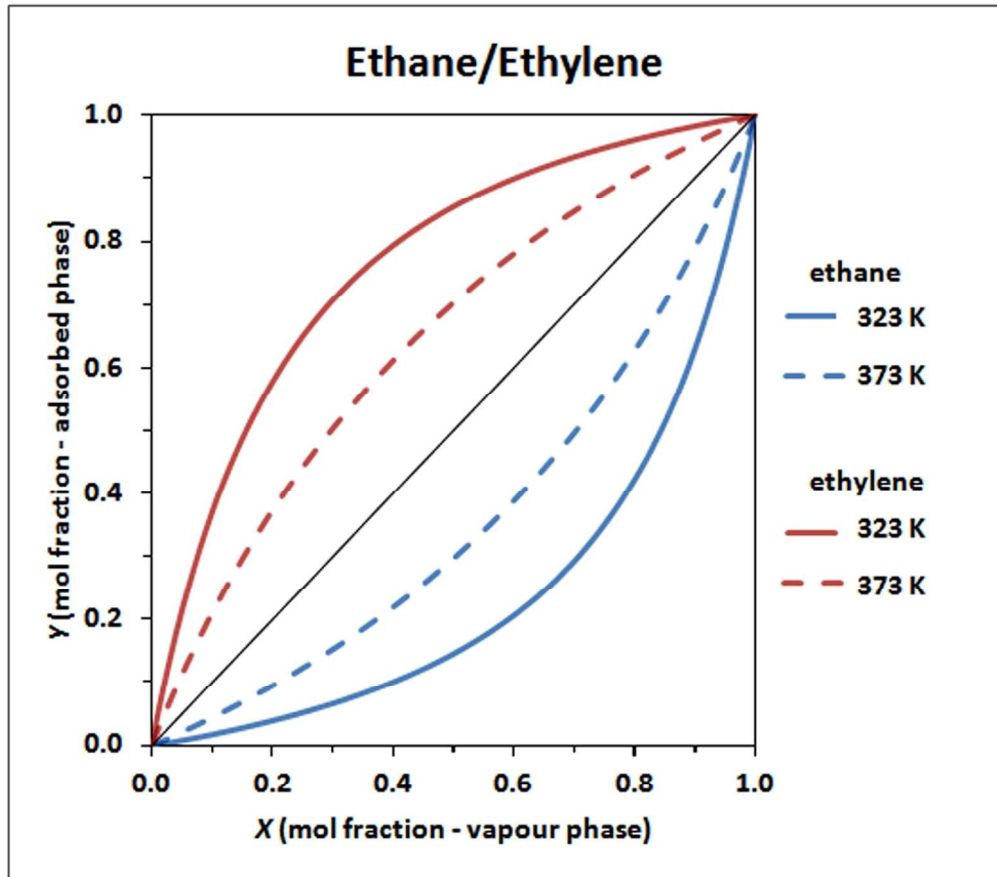


Figure 8 - Binary component equilibrium diagrams at different temperatures.
122x107mm (300 x 300 DPI)

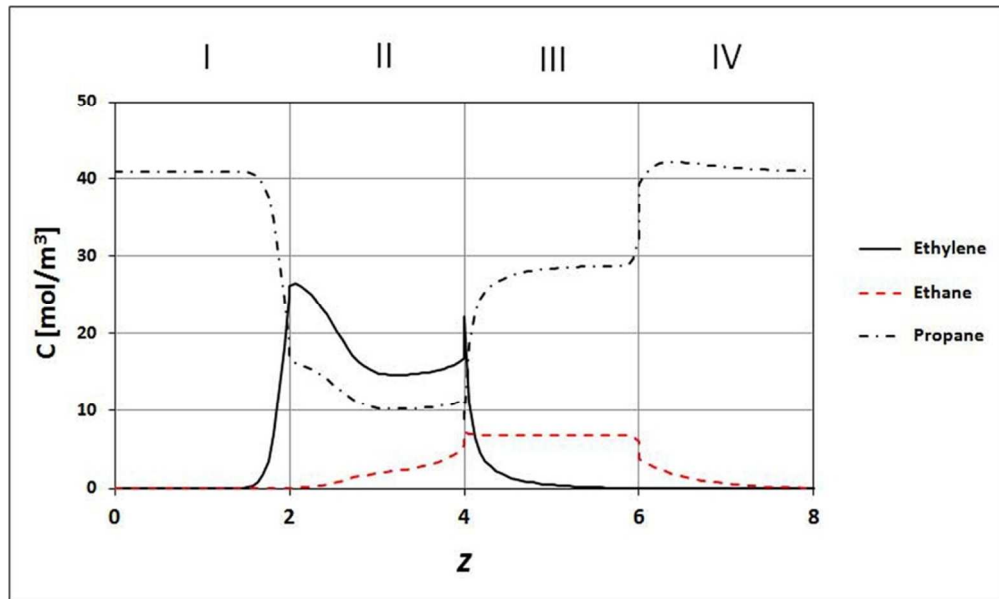


Figure 9 - Concentration profile along the unit for the selected operating point using propane as desorbent.
83x49mm (300 x 300 DPI)

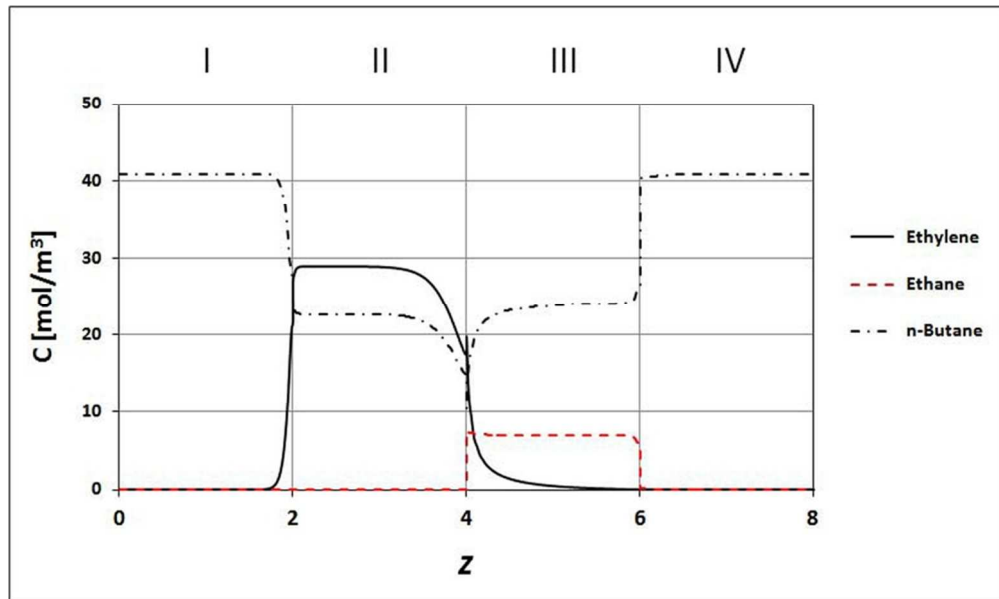
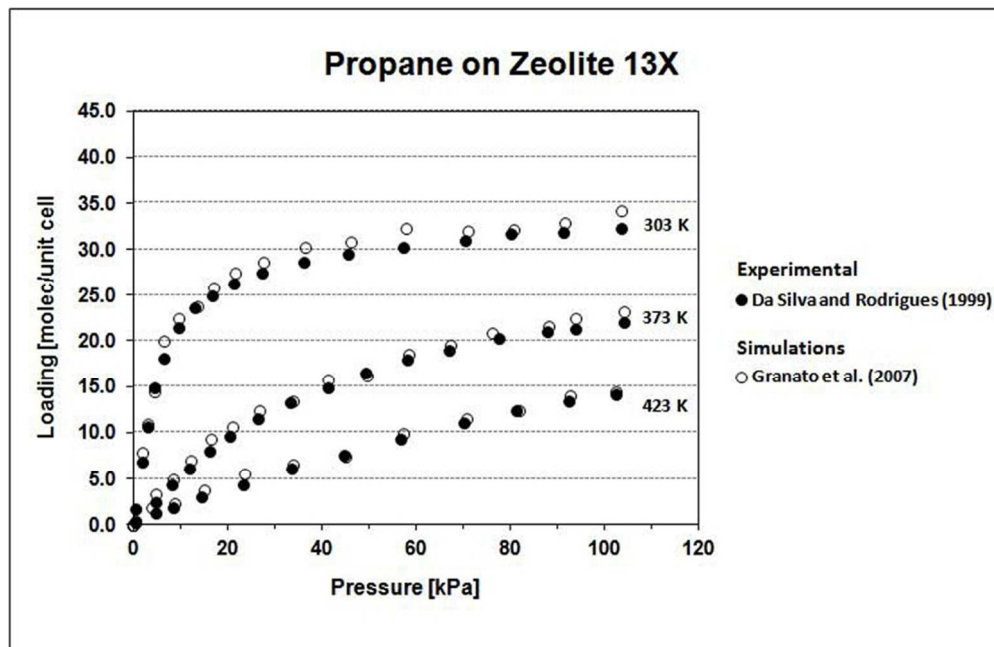
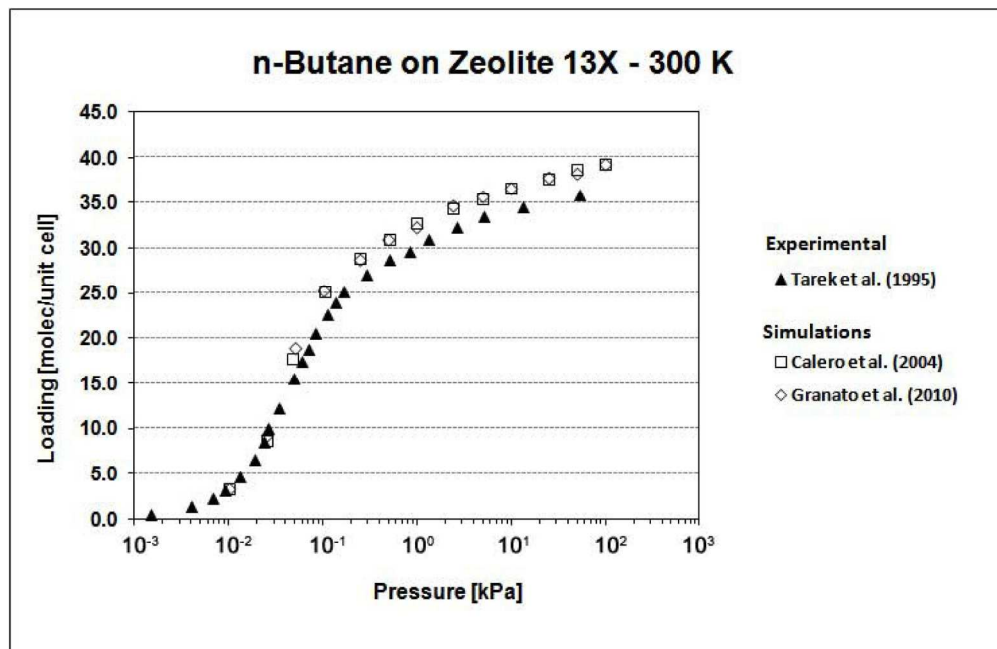


Figure 10 - Concentration profile along the unit for the selected operating point using n butane as desorbent.
83x49mm (300 x 300 DPI)



90x58mm (300 x 300 DPI)



29 Figure S1 – Isotherms of propane(a) and n-butane(b). Taken from Granato et al. (2007, 2010).
30 170x110mm (300 x 300 DPI)